Meta Gene 3 (2015) 43–49

Contents lists available at ScienceDirect

Meta Gene

Investigation of molybdenum cofactor deficiency due to *MOCS2* deficiency in a newborn baby

Matthew Edwards [a,b,*], Juliane Roeper [c,d], Catherine Allgood [a,b], Raymond Chin [a,b], Jose Santamaria [c,d], Flora Wong [e,f], Guenter Schwarz [c,d], John Whitehall [a,b]

[a] Department of Paediatrics, Campbelltown Hospital, Campbelltown, NSW, Australia
[b] Department of Paediatrics, School of Medicine, University of Western Sydney, Campbelltown, NSW, Australia
[c] Colbourne Pharmaceuticals GmbH, Viktoriaweg 7, 53859 Niederkassel, Germany
[d] University of Cologne, Germany
[e] Monash Newborn, Level 5, 246 Clayton Road, Clayton, Victoria 3168, Australia
[f] The Ritchie Centre, Department of Paediatrics, Faculty of Medicine, Nursing and Health Sciences, Monash University, Wellington Road, Clayton, Victoria 3800, Australia

ARTICLE INFO

Article history:
Received 22 June 2014
Revised 3 December 2014
Accepted 16 December 2014
Available online 31 January 2015

Keywords:
Molybdenum cofactor deficiency
MOCS2A
Metabolic encephalopathy

ABSTRACT

Background: Molybdenum cofactor deficiency (MOCD) is a severe autosomal recessive neonatal metabolic disease that causes seizures and death or severe brain damage. Symptoms, signs and cerebral images can resemble those attributed to intrapartum hypoxia. In humans, molybdenum cofactor (MOCO) has been found to participate in four metabolic reactions: aldehyde dehydrogenase (or oxidase), xanthine oxidoreductase (or oxidase) and sulfite oxidase, and some of the components of molybdenum cofactor synthesis participate in amidoxime reductase. A newborn girl developed refractory seizures, opisthotonus, exaggerated startle reflexes and vomiting on the second day of life. Treatment included intravenous fluid, glucose supplementation, empiric antibiotic therapy and anticonvulsant medication. Her encephalopathy progressed, and she was given palliative care and died aged 1 week. There were no dysmorphic features, including ectopia lentis but ultrasonography revealed a thin corpus callosum.

Objectives: The aim of this study is to provide etiology, prognosis and genetic counseling.

* Corresponding author at: Department of Paediatrics, Camden and Campbelltown Hospitals, Post Office Box 149, Campbelltown NSW 2560, Australia. Tel.: +61 40 2364080; fax: +61 246343650.
E-mail addresses: M.Edwards@uws.edu.au (M. Edwards), juliane.roeper@web.de (J. Roeper), Catherine.Allgood@sswahs.nsw.gov.au (C. Allgood), Raymond.Chin@sswahs.nsw.gov.au (R. Chin), hispania76@gmail.com (J. Santamaria), flora.wong@monash.edu (F. Wong), gschwarz@uni-koeln.de (G. Schwarz), John.Whitehall@uws.edu.au (J. Whitehall).

http://dx.doi.org/10.1016/j.mgene.2014.12.003

Methods: Biochemical analysis of urine, blood, Sanger sequencing of leukocyte DNA, and analysis of the effect of the mutation on protein expression.

Results: Uric acid level was low in blood, and S-sulfo-L-cysteine and xanthine were elevated in urine. Compound Z was detected in urine. Two MOCS2 gene mutations were identified: c.501 + 2delT, which disrupts a conserved splice site sequence, and c.419C > T (pS140F). Protein expression studies confirmed that the p.S140F substitution was pathogenic. The parents were shown to be heterozygous carriers.

Conclusions: Mutation analysis confirmed that the MOCD in this family could not be treated with cPMP infusion, and enabled prenatal diagnosis and termination of a subsequent affected pregnancy.

Introduction

Molybdenum participates in several enzyme reactions including xanthine oxidase, aldehyde oxidase and sulfite oxidase. The molybdenum cofactor (MOCO) is essential for the activity of these enzymes and is associated with amidoxime reductase in mitochondria. MOCO deficiency (MOCD) causes a severe progressive metabolic encephalopathy with neonatal convulsions, spasticity, opisthotonus, brain atrophy, altered facial morphology and severe developmental disability, spherophakia and dislocated lenses in survivors, associated with deficiency of both xanthine oxidase and sulfite oxidase. Cerebral MRI findings can resemble those of severe hypoxic–ischemic encephalopathy (Topcu et al., 2001). Histopathology of the brain shows severe loss of neocortical neurons, gliosis and areas of cystic necrosis in white matter, also seen in sulfite oxidase deficiency, suggesting that deficiency of sulfite oxidase causes much of the cerebral pathology. The *MOCS1A* and *MOCS1B* genes encode an enzyme complex that forms cyclic pyranopterin monophosphate (cPMP) from GTP. The *MOCS2A* and *MOCS2B* gene product, in association with a protein encoded by *MOCS3*, convert cPMP to molybdopterin (MPT). cPMP is deficient or absent when there are mutations in the *MOCS1* gene, while its oxidation product, compound Z, is detectable in urine when there are *MOCS2* mutations (Fig. 1).

The *GEPHYRIN* gene product adenylates MPT and adds molybdenum to form MOCO. When urine amino acids are screened on suspicion of a metabolic disease, an elevated S-sulfo-L-cysteine level suggests either sulfite oxidase deficiency or MOCD. An elevation of urine xanthine and low blood uric acid indicate an additional deficiency of xanthine oxidase due to MOCD. Patients with MOCS1A or MOCS1B deficiency have been treated with a stable injectable form of cPMP (Hitzert et al., 2012; Veldman et al., 2010), but with MOCS2 mutations supplementation with cPMP is ineffective. Pyridoxal-5-phosphate is sequestered by elevated levels of

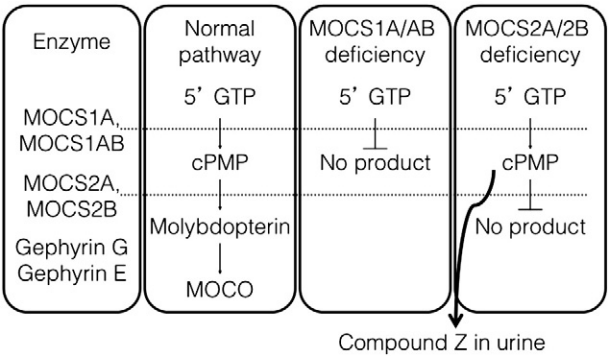

Fig. 1. Normal and MOCS1- or MOCS2-deficient pathways for MOCO synthesis. MOCS2 deficiency can be distinguished from MOCS1 deficiency by the detection of compound Z, oxidation product of cPMP, in urine.

the cyclic form of alpha-amino adipic semialdehyde (piperideine-6-carboxylate) in MOCD, so seizures in MOCD might respond to pyridoxine supplementation (Struys et al., 2012).

Subject

A 3.2 kg full term newborn girl with Apgar scores 9 at 1 min and 5 min appeared well until day 2 when refractory seizures, opisthotonus, startle reflexes and vomiting developed. The pregnancy and family history were unremarkable; the parents were of Samoan and Caucasian origin. Despite treatment with intravenous glucose-saline, phenobarbitone and phenytoin, the baby became obtunded and died aged 7 days. There were no dysmorphic features or ectopia lentis. Cranial ultrasound MRI showed a thin anterior corpus callosum and MRI showed severe hypoplasia of its body and splenium; there was a slight parallel appearance of the lateral ventricles with mild prominence of the trigone and temporal horns. There was subtle loss of gray/white matter differentiation and cerebral edema with attenuation of surface CSF spaces. A subependymal cyst projected within the body of the left lateral ventricle. The deep cerebral veins, the vein of Galen and the internal cerebral veins were dilated. A dilated serpiginious vein connected the superior sagittal sinus and vein of Galen instead of the usual straight sinus and could indicate a persistent embryonic vein. The weights and measurements were in keeping with the gestational age at autopsy, which confirmed normal external morphology and thinning of the corpus callosum, cerebral edema and congested tortuous meningeal vessels. Histological findings included extensive neocortical neuronal loss, spongiosis and gliosis. No abnormalities were found in other organs.

Methods

Uric acid, S-sulfo-L-cysteine and xanthine in urine were measured by direct-injection electrospray tandem mass spectrography (Veldman et al., 2010). Urine sulfite was measured by a semi-quantitative dipstick test (Merckoquant test sulfite, Merck Chemicals, Darmstadt, Germany). Urine compound Z was quantified by high-performance liquid chromatography. Mutations in MOCS2B were identified by PCR amplification of exons and neighboring intronic sequences of leukocyte genomic DNA from the patient and her parents and Sanger sequencing. MOCS2A and MOCS2B wild-type (WT) proteins and the MOCS2B-S140F variant were recombinantly expressed in *Escherichia coli* and purified to homogeneity. The small subunit of MPT synthase, MOCS2A, was expressed and purified as intein-fusion protein with a chitin-domain for subsequent affinity purification and eluted with ammonium sulfide, resulting in the release of activated MOCS2A protein with a thiocarboxylated C-terminal tail (Gutzke et al., 2001). MOCS2B wildtype and the MOCS2B-S140F variant were cloned into pET15b, expressed in *E. coli* BL21 and purified by ammonium sulfate precipitation and subsequent gelfiltration using Superdex 200 size exclusion column. Changes in three-dimensional structure of the mutant protein were analyzed by circular dichroism spectroscopy (Rudolph et al., 2001). Complex formation of MPT synthase was analyzed by isothermal titration calorimetry using MOCS2A and either WT MOCS2B or the MOCS2B-S140F variant. In vitro MPT synthesis rates were quantified as a function of the concentration of small MPT synthase subunit MOCS2A (Llamas et al., 2004).

Results

Uric acid levels in urine were low during life and at autopsy, and urine xanthine was elevated, while the level of compound Z which is normally undetectable in urine was found to be elevated (data not shown). Urine S-sulfocysteine (44 μmol/l) and S-sulfocysteine:creatinine ratio (231 μmol/mmol creatinine) were markedly elevated.

Two novel mutations of the MOCS2 gene in DNA from blood of the patient were predicted to impair mRNA synthesis or enzyme activity. One, c.419C > T (p.S140F) encoded a substitution of phenylalanine for serine and the other, c.501 + 2delT is predicted to disrupt a splice site. Each parent was heterozygous for one of the two mutations.

In silico analysis using the crystal structure of bacterial MPT synthase predicted the location of S140 at the end of β-stand 6, which is part of a highly conserved sequence motif forming the active site within the MOCS2B (*E. coli* MoaE) and being involved in binding the C-terminal end of MOCS2A (*E. coli* MoaD). The exchange of the polar serine residue to the much larger, hydrophobic phenylalanine presumably influences the

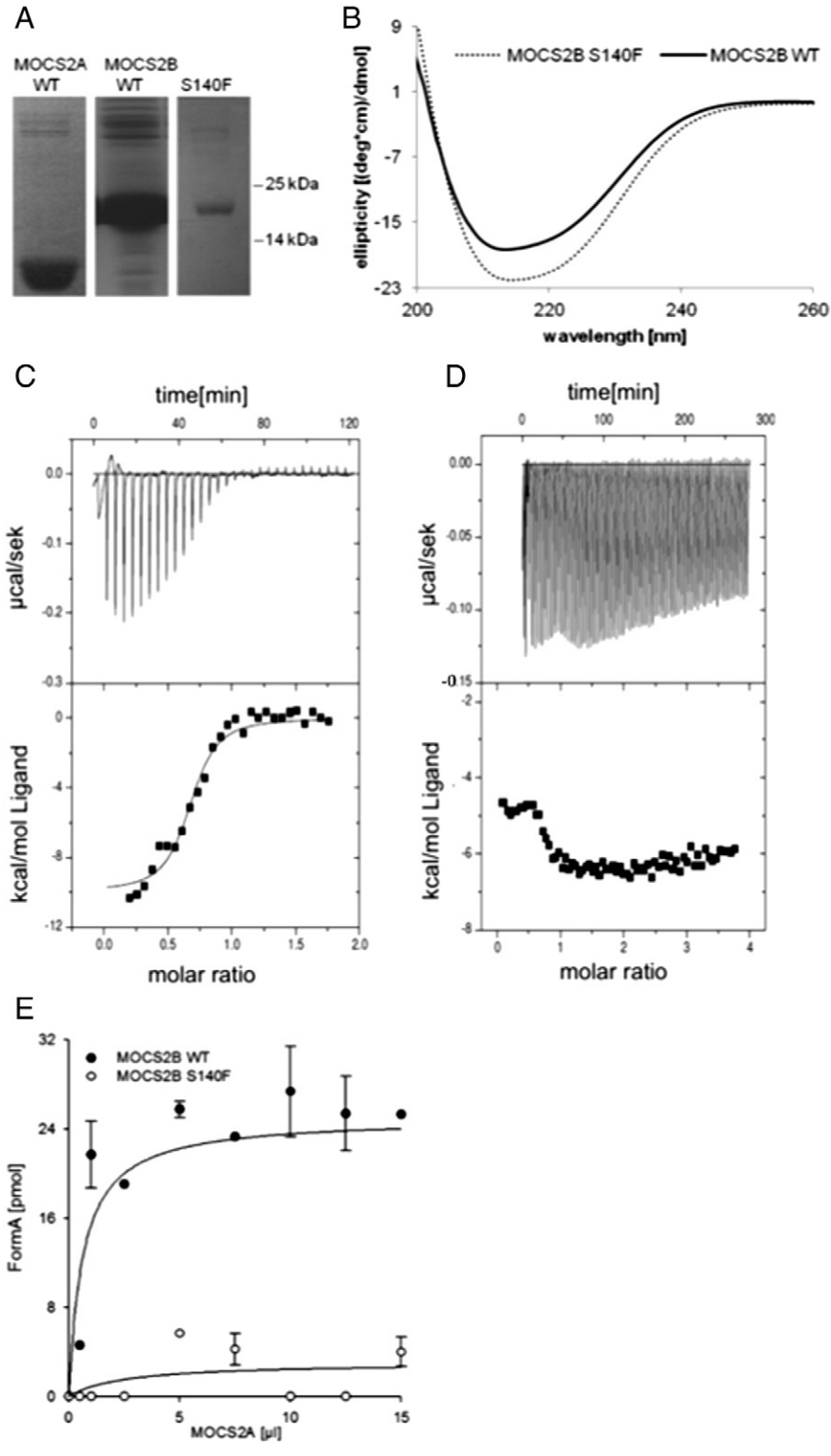
A
MOCS2A WT
MOCS2B WT
S140F
25 kDa
14 kDa
B
MOCS2B S140F
MOCS2B WT
ellipticity [(deg*cm)/dmol]
wavelength [nm]
C
time[min]
µcal/sek
kcal/mol Ligand
molar ratio
D
time[min]
µcal/sek
kcal/mol Ligand
molar ratio
E
MOCS2B WT
MOCS2B S140F
FormA [pmol]
MOCS2A [µl]

stability of the central β-sheet of MOCS2B and the overall assembly of the heterotetrameric MPT synthase complex.

Following expression and purification, the total yield of MOCS2B-S140F was much lower than that for WT MOCS2B (Fig. 2A). Consistently, circular dichroism spectroscopy revealed an alteration in the protein folding, given that between 210 and 220 nm a more negative signal was recorded, which suggests changes in the content of helical structures in MOCS2B-S140F (Fig. 2B). These might influence either the oligomerization between two MOCS2B protomers or the interaction with the small subunit (MOCS2A). Therefore, we analyzed the complex formation of MPT synthase by isothermal titration calorimetry using MOCS2A and either WT MOCS2B or the MOCS2B-S140F variant. While in the presence of WT MOCS2A an effective complex formation associated with a saturation of heat release was observed (Fig. 2C), only minor heat release peaks were seen with MOCS2B-S140F (Fig. 2D) suggesting a severely affected interaction between both subunits, which could not be quantified. Note that WT MOCS2B binds MOCS2A with a $K_d = 0.36 \pm 0.047$ μM (Fig. 2C). This finding identifies a defective association of both MPT synthase subunits as a major disease-causing mechanism.

Finally, we determined in vitro MPT synthesis rates as a function of the concentration of small MPT synthase subunit MOCS2A. While WT MOCS2B showed an effective MPT synthesis (determined by the oxidation product FormA, Fig. 2E), MOCS2B-S140F was only able to produce low levels of MPT at high concentrations of MOCS2A.

Discussion

The differential diagnosis of MOCD includes deficiency of sulfite oxidase and pyridoxine-dependent epilepsy (Struys et al., 2012). MOCD can be associated with a number of morphological abnormalities of the brain and face. This patient had no external morphological abnormalities. It is important to emphasize that some of the reported changes can be similar to those seen in neonates with hypoxic–ischemic encephalopathy, so metabolic investigations should not be neglected in cases of presumed intrapartum hypoxia (Topcu et al., 2001). Investigations should include screening of amino acids in urine, which would identify high levels of S-sulfo-L-cysteine in MOCD, associated with high urinary xanthine and low levels of plasma uric acid. The detection in urine of compound Z confirms the diagnosis of MOCS2 deficiency, and facilitates decisions about treatment. Exogenous cPMP only works in cases with MOCS1 deficiency who cannot synthesize cPMP, and could potentially slow or stop the progression of disease (Veldman et al., 2010), although seizures and "cramped synchronized general movements" have been observed on day 1 in a baby diagnosed prenatally with a MOCS1 mutation (Hitzert et al., 2012), so it is possible that irreversible brain damage occurs prenatally. In this case, protein expression experiments confirmed that the S140F mutation severely reduces complex formation of MPT synthase. As some residual activity is detectable in vitro, a milder presentation with low levels of enzyme activity might be considered in this case. In vitro analysis of expression of the allele containing the splice site mutation was not possible for this patient, although the wild type human sequence at both c.419 and c.501 + 2 is conserved in several species (Table 1) (Anonymous, 2014). Mutation analysis enabled prenatal genetic diagnosis and termination of a subsequent affected pregnancy. Biochemical testing for recurrence in a future pregnancy could include measurement of S-sulfo-L-cysteine level or sulfite oxidase activity in chorion villus cells, or of S-sulfo-L-cysteine in amniotic fluid. Mutation analysis reassured the parents that treatment with exogenous cPMP was not indicated, as it has only been shown to help babies with MOCS1 mutations. The child died before the potential benefit of pyridoxine supplementation was published (Struys et al., 2012).

Acknowledgments

We thank the parents of the baby for their support with this publication.

Fig. 2. Protein expression studies, S140F mutation. A: SDS-PAGE analysis of expression of purified recombinant wild type MOCS2A (left lane) and MOCS2B (middle lane), and MOCS2B S140F mutation (right lane). B: circular dichroism spectroscopy showing more negative signal for MOCS2B S140F at a wavelength of 210–220 nm. C: isothermal titration calorimetry using MOCS2A and WT MOCS2B, showing the expected heat release on formation of active MPT synthase. D: isothermal titration calorimetry using MOCS2A and mutant MOCS2B-S140F, showing abnormal minor heat release peaks on formation of MPT synthase. E: In vitro MPT synthesis rates as a function of the concentration of small MPT synthase subunit MOCS2A. WT MOCS2B (filled circles) yielded expected amounts of the MPT oxidation product, FormA, while use of the mutant protein MOCS2B-S140F (open circles) significantly reduced synthesi.

Table 1

MOCS2 gene: GRCh38 assembly genomic nucleotide number			53100497 ↓								53100488 ↓			53100420 ↓																						53100400 ↓		
Human coding strand sequence		5′	G	T	G	T	C	C	T	C	A	T	A	C	C	T	T	T	T	T	C	C	A	T	T	C	A	A	T	T	C							3′
Protein sequence (p.)			139V			140S			141S			I	165W			166K			167K			Intron 6																
Complementary strand sequence	Human	3′	C	A	C	A	G	G	A	G	T	A	T	G	G	A	A	A	A	A	G	G	T	A	A	G	T	T	A	A	G							5′
	Mouse		C	C	C	A	G	A	A	G	T	A	T	G	G	A	A	A	A	A	G	G	T	G	A	G	T	G	A	G	G							
	Heterocephalus glaber		C	A	C	A	G	G	A	G	T	A	T	G	G	A	A	A	A	A	G	G	T	G	A	G	T	T	A	A	G							
	Mustela futorius		C	A	C	A	G	G	A	G	T	A	T	G	G	A	A	A	A	A	G	T	T	A	A	G												
	Ascaris lumbricoides		C	C	C	A	G	G	A	G	T	A	T	G	G	A	A	A	A	A	G	G	T	A	A	G	T	T	A	A	G							
Coding sequence number (c.)			416			419			422				494			497			500			↑ c.501+2																

Evolutionary conservation of wild-type sequence at c.419 and c.501 + 2 of MOCS2 (bold borders).

References

Anonymous, 2014. Reference NC_000005.10. http://blast.ncbi.nlm.nih.gov/Blast.cgi. National Center for Biotechnology Information, National Library of Medicine.

Gutzke, G., Fischer, B., Mendel, R.R., Schwarz, G., 2001. Thiocarboxylation of molybdopterin synthase provides evidence for the mechanism of dithiolene formation in metal-binding pterins. J. Biol. Chem. 276, 36268–36274.

Hitzert, M.M., Bos, A.F., Bergman, K.A., Veldman, A., Schwarz, G., Santamaria-Araujo, J.A., Heiner-Fokkema, R., Sival, D.A., Lunsing, R.J., Arjune, S., Kosterink, J.G., van Spronsen, F.J., 2012. Favorable outcome in a newborn with molybdenum cofactor type A deficiency treated with cPMP. Pediatrics 130, e1005–e1010.

Llamas, A., Mendel, R.R., Schwarz, G., 2004. Synthesis of adenylated molybdopterin: an essential step for molybdenum insertion. J. Biol. Chem. 279, 55241–55246.

Rudolph, M.J., Wuebbens, M.M., Rajagopalan, K.V., Schindelin, H., 2001. Crystal structure of molybdopterin synthase and its evolutionary relationship to ubiquitin activation. Nat. Struct. Biol. 8, 42–46.

Struys, E.A., Nota, B., Bakkali, A., Al Shahwan, S., Salomons, G.S., Tabarki, B., 2012. Pyridoxine-dependent epilepsy with elevated urinary alpha-amino adipic semialdehyde in molybdenum cofactor deficiency. Pediatrics 130, e1716–e1719.

Topcu, M., Coskun, T., Haliloglu, G., Saatci, I., 2001. Molybdenum cofactor deficiency: report of three cases presenting as hypoxic–ischemic encephalopathy. J. Child Neurol. 16, 264–270.

Veldman, A., Santamaria-Araujo, J.A., Sollazzo, S., Pitt, J., Gianello, R., Yaplito-Lee, J., Wong, F., Ramsden, C.A., Reiss, J., Cook, I., Fairweather, J., Schwarz, G., 2010. Successful treatment of molybdenum cofactor deficiency type A with cPMP. Pediatrics 125, e1249–e1254.